

# Contribution of underlying terrain to sand dunes: evidence from the Qaidam Basin, Northwest China

LI Jiyan<sup>1\*</sup>, QU Xin<sup>1</sup>, DONG Zhibao<sup>2</sup>, CAI Yingying<sup>1</sup>, LIU Min<sup>1</sup>, REN Xiaozong<sup>1</sup>, CUI Xujia<sup>1</sup>

<sup>1</sup> School of Geography Science, Taiyuan Normal University, Jinzhong 030619, China;

<sup>2</sup> School of Geography and Tourism, Shaanxi Normal University, Xi'an 710119, China

**Abstract:** Underlying terrain strongly influences dune formation. However, the impacts of underlying terrain on the dune formation are poorly studied. In the present research, we focused on dunes that formed in the alluvial fans and dry salt flats in the Qaidam Basin, Northwest China. We quantified the dunes' sediment characteristics on different types of underlying terrain and the terrain' effects on the surface quartz grains by analyzing grain-size distribution, soluble salt contents and grain surface micro-textures. Results showed that barchan dunes were dominated by medium sands with a unimodal frequency distribution, whose peak corresponded to the saltation load. Linear dunes were mainly composed of fine sands with a bimodal frequency distribution, whose main peak represented the saltation load, and whose secondary peak represented the modified saltation or suspension load. Sand was transported from source area by running water (inland rivers) over short distances and by wind over relatively longer distances. Thus, quartz grains had poor roundness and were dominated by sub-angular and angular shapes. Surface micro-textures indicated that dune sands were successively transported by exogenic agents (glaciation, fluviation and wind). Soluble salt contents were low in dunes that developed in the alluvial fans, which represented a low-energy chemical environment, so the grain surface micro-textures mainly resulted from mechanical erosion, with weak micro-textures formed by SiO<sub>2</sub> solution and precipitation. However, soluble salt contents were much higher in dunes that developed in the dry salt flats, which indicated a high-energy chemical environment. Therefore, in addition to micro-structures caused by mechanical erosion, micro-textures formed by SiO<sub>2</sub> solution and precipitation also well developed. Our results improve understanding of the sediment characteristics of dune sands and the effects of underlying terrain on dune development in the Qaidam Basin, China.

**Keywords:** dune; grain-size distribution; soluble salts; surface micro-texture; Qaidam Basin

## 1 Introduction

Sandy deserts are mainly located in the world's hyper-arid and arid areas, as well as in some coastal areas. Deserts represent the regional deposition centers for sediments and contain a range of types and scales of sand dunes, as well as large areas of sand sheets and wide inter-dune areas (Lancaster, 2013). Regional sand transport system consists of three components, i.e., sand source areas, transport pathways and depositional sinks (Lancaster et al., 2015). The main factors that

---

\*Corresponding author: LI Jiyan (E-mail: jyli@tynu.edu.cn)

Received 2021-08-08; revised 2021-12-14; accepted 2021-12-22

© Xinjiang Institute of Ecology and Geography, Chinese Academy of Sciences, Science Press and Springer-Verlag GmbH Germany, part of Springer Nature 2021

control these components include the supply of sand, the availability of erodible surface sand and the wind's transport capacity (Kocurek and Lancaster, 1999). Regional aeolian landform studies not only demonstrate the morpho-dynamic processes that control the development of different dune types (Dong et al., 2004, 2010), but also clarify the characteristics of dune sediments to reveal their provenance and transport pathways (Muhs et al., 2003; Li et al., 2015; Qian et al., 2020).

These issues have been mainly addressed by comparing the mineral and chemical element composition of dune sands with the surface sediments of potential source areas, and this approach has been successfully applied in studies of sediment provenance in deserts around the world (Xu et al., 2010; Scheidt et al., 2011; Garzanti et al., 2013; Hu and Yang, 2016; Zhang et al., 2020). These studies indicated that the clastic materials were produced by weathering and denudation. A region's fluvial, alluvial and lacustrine sediments can provide materials for the formation of sandy deserts (Wu, 2010). However, it's still necessary to clarify the effects of exogenic agents other than water and wind during the transport of dune sands from source areas to sinks in sandy deserts, as well as the effects of underlying terrain on the processes that lead to the formation of dune sands.

Desert in the Qaidam Basin is the sixth-largest desert with the highest elevation in China, and includes large areas of wind erosional and depositional landforms (Zhu et al., 1980). Simple dunes and sporadic dunes are dominated in the desert. The provenance and dominant transport pathways in the basin are not yet well understood. Aeolian sands are mainly composed of quartz and feldspar, with the quartz sand grains most resistant to physical and chemical alteration. In contrast, feldspar is softer and more vulnerable to physical and chemical erosion, and a decrease in the feldspar content provides evidence of the sediment's post-formation evolution. Thus, quartz sand grains bear abundant information on the sedimentary environment where they formed (Bristow and Livingstone, 2019). Aeolian sands play an important role in research on the evolution of the Quaternary paleogeographic environment in the Qaidam Basin, especially since the Last Glacial Maximum (Zeng et al., 2003; Yu and Lai, 2014; Yu et al., 2015).

Chen and Lü (1959) proposed that aeolian sands in the Qaidam Basin may originated from the Tarim Basin. However, their conclusion lacked confirmation by subsequent experimental evidence. More recent research suggested that mineral assemblage characteristics of dune sands in the basin resulted from transport of piedmont alluvial–diluvial deposits from the surrounding mountains and the transport of exposed lacustrine sediments after drying of the Qarhan Salt Lake (Bao and Dong, 2015). By analyzing the geochemical element composition of dune sands in different grain-size fractions, Du et al. (2018) found that coarse components (75–500  $\mu\text{m}$ ) were derived from local fluvial and alluvial–diluvial deposits, whereas fine components (<75  $\mu\text{m}$ ) were derived from the Tarim Basin. Based on the characteristics of geochemical elements and mineral assemblages in dune sands and surface sediments from potential source areas, Li et al. (2018, 2020) found that both gobi surface sediments and yardang corridor sands could provide sandy material to support the development of linear dunes on the northern margin of the Qarhan Salt Lake, which is a residual of ancient lake. These sands were derived from granite and granodiorite rocks in the Qilian Mountains. However, there have been few studies on the surface micro-textures of quartz sand grains that provide evidence of their provenance and transport pathways (Dong et al., 2017a).

Linear and barchan dunes are the most common dunes in the Qaidam Basin. The former are mainly found in the dry salt flats around the Qarhan Salt Lake, whereas the latter are mostly found in the alluvial fans in the piedmont of basin's surrounding mountains (Zhang et al., 2018). Given our summary of previous research in this area, we focused on linear and barchan dunes that developed on different types of underlying terrain (salt flats vs. alluvial fans) in the Qaidam Basin, and analyzed their sedimentary characteristics (grain-size, soluble salt content, roundness and surface micro-texture) of quartz sand grains. We did not study the feldspar particles because their vulnerability to physical and chemical erosion made them an unreliable clue to the origins of

particles. Furthermore, we compared the differences of sedimentary characteristics between dune sands that accumulated in the salt flats and alluvial fans, and discuss the influence of underlying terrain on these aeolian sands.

## 2 Materials and methods

### 2.1 Study area

The Qaidam Basin is the largest intermontane fault basin on the northeastern Tibetan Plateau, China. It is encircled by the Kunlun Mountains in the south and west, the Altun Mountains in the northwest, and the Qilian Mountains in the northeast (Fig. 1). Elevation of the surrounding mountains ranges from 4000 to 5000 m a.s.l., versus an average of 2800 m a.s.l. for the floor of the basin, which covers an area of  $12 \times 10^4 \text{ km}^2$ . As a typical endorheic basin, the Qaidam Basin is characterized by a convergent drainage system, with rivers that originate in the surrounding mountains and feed the saline lakes in the central-southern part of the basin. The highest elevation and the largest yardang field in China occurred in northwestern Qaidam Basin (Li et al., 2016). The basin has a hyper-arid climate, with mean annual precipitation ranging from 100 mm in the southeast to less than 20 mm in the northwest, with mean annual potential evaporation that reaches more than 100 times the precipitation (Han et al., 2014). Another climate characteristic of the Qaidam Basin is the frequent occurrence of sand and dust storms, especially from March to May, with a frequency of 40 d/a under the influence of prevailing northerly and northwesterly winds (Yu and Lai, 2012).

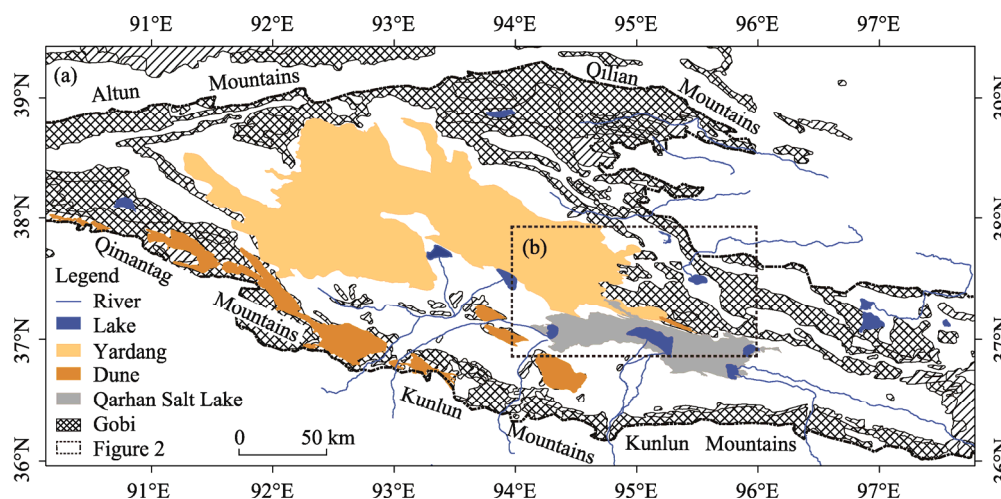


**Fig. 1** (a), geographical settings of the Qaidam Basin; (b), location of samples.

Aeolian landforms in the Qaidam Basin cover up to  $3.4 \times 10^4 \text{ km}^2$ , with the aeolian depositional landforms covering  $1.3 \times 10^4 \text{ km}^2$ , and the aeolian erosional landforms covering  $2.1 \times 10^4 \text{ km}^2$  (Dong et al., 2017b). Dunes in the basin have mainly developed on two types of underlying terrain. The first comprises alluvial fans, especially in the piedmont of the Qimantagh Mountains inward basin (Fig. 1). Dunes that formed in the alluvial fans are dominated by barchans and barchan chains, with dunes reaching 5 to 10 m in height; and the dunes migrate 20 m/a in the prevailing wind direction (Zhu et al., 1980). The second type of underlying terrain comprises dry salt flats that surround the Qarhan Salt Lake. These regions are dominated by linear dunes, with heights reaching 30 m (Zhou et al., 2012). The linear dunes are much more stable than the barchans, and their elongation rate attains 4–10 m/a (Qian, 1986).

### 2.2 Methods

Based on the differences between two types of underlying terrain, we studied barchan dunes (BD01 and BD02) that developed on the north-slope alluvial fans of the Lvliang Mountains, and

linear dunes (LD01 to LD03) and barchan dunes (BD03) that developed on the salt flats around the Qarhan Salt Lake (Fig. 2). We collected surface sediment samples from the barchans' crest (Fig. 3a), and collected samples from linear dunes along a topography transect perpendicular to dune orientation at the following positions: the base of SSW (south-southwest) slope, the crest, the base of NNE (north-northeast) slope and inter-dune area (Fig. 3b). We collected a total of 15 samples: one crest sample at each barchan site and four samples at each of the linear dune site. Each sample contained the surface sediments in an area of 20 cm×20 cm to a depth of 2 cm. Each sample weighed about 500 g.

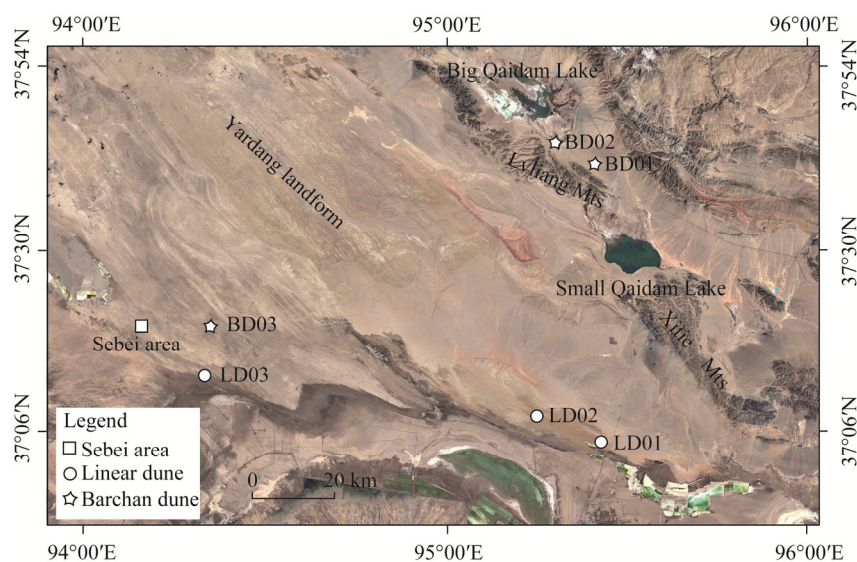


**Fig. 2** Location and sampling position of the study dunes

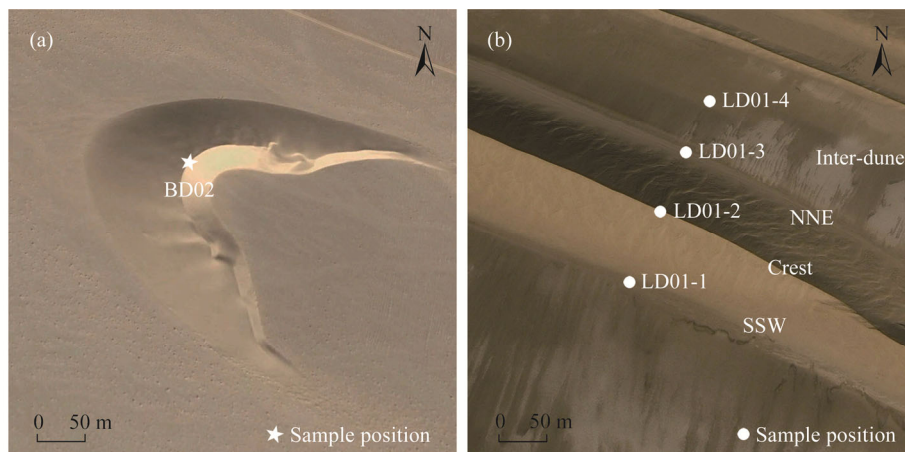


**Fig. 3** Sample positions of dune surface sediments for barchan (BD, a) and linear (LD, b) dunes. SSW, south-southwest; NNE, north-northeast.

We analyzed the grain-size distribution of samples using a Malvern Mastersizer 2000 (Malvern Instruments, Malvern, UK) at the School of Geography and Tourism, Shaanxi Normal University, China. Grain-size parameters were the mean grain-size ( $M_z$ ,  $\phi$ ), sorting ( $\sigma_1$ ), skewness ( $SK_1$ ) and kurtosis ( $K_g$ ). We calculated their values graphically according to the methods proposed by Folk and Ward (1957). Soluble salt content was calculated from the mass of dried residue. We examined the surface micro-texture of quartz sand grains using a Mineral Liberation Analyzer (MLA 650, FEI Company, Hillsboro, USA). We had totally observed 476 quartz sand grains of their roundness and surface micro-textures for the 15 samples. Roundness of quartz sand grains



was determined following the method described by Powers (1953), and surface micro-texture was interpreted by Krinsley and Doornkamp (1973) and Xie (1984).

### 3 Results

#### 3.1 Grain-size characteristics

##### 3.1.1 Grain-size distribution

Grain-size distribution of sediments is not only affected by sand source, but also influenced by the changes that occur during subsequent transport and deposition processes. Contents of different grain-size fractions differed greatly among the dune and inter-dune deposits as well as between different types of dunes (Table 1). Dune surface sediments were dominated by fine and medium sands, with average contents of 30.49% and 28.05%, respectively, versus 15.33% and 11.46%, respectively, for coarse and very fine sands. In contrast, inter-dune sediments between linear dunes were dominated by silt, with an average content of 28.35%, followed by similar average contents of fine (18.25%) and very fine sands (17.60%), respectively. In barchan dunes, medium sand was the dominant size category, with an average content of 59.32%, and mean contents of fine and coarse sands were 28.26% and 11.36%, respectively. Fine sand content was the highest in linear dune sediments, with an average value of 31.24%, followed by medium sand (17.63%), with similar contents of coarse and very fine sands (16.66% and 15.15%, respectively).

**Table 1** Grain-size fractions and soluble salt contents for dune surface sediments

Sample	Clay (%)	Silt (%)	VFS (%)	FS (%)	MS (%)	CS (%)	VCS (%)	Soluble salt (%)	$M_z$ ( $\phi$ )	$\sigma_1$	$SK_1$	$K_g$
BD01	0.00	0.00	0.13	36.51	61.10	2.13	0.00	0.13	1.84	0.44	0.01	0.95
BD02	0.00	0.00	0.68	36.92	57.75	4.62	0.00	0.03	1.83	0.51	0.01	0.95
BD03	0.00	0.91	0.41	11.36	59.10	27.32	0.00	0.90	1.35	0.56	0.04	0.96
LD01-1	7.76	22.80	15.76	24.68	17.83	2.03	0.00	9.14	3.65	2.21	0.46	1.12
LD01-2	7.28	12.74	26.88	39.87	8.15	0.00	0.00	5.09	3.57	1.82	0.60	2.15
LD01-3	5.43	12.45	14.24	33.24	24.90	2.24	0.00	7.51	2.92	1.78	0.50	1.77
LD01-4	12.02	33.42	19.29	16.34	7.92	0.18	0.00	10.83	4.56	2.37	0.36	1.03
LD02-1	0.42	1.68	9.46	23.02	20.51	28.59	15.33	0.99	1.36	1.29	0.12	0.76
LD02-2	1.58	3.36	16.92	69.72	6.99	0.00	0.00	1.42	2.65	0.72	0.30	2.12
LD02-3	0.17	1.31	3.19	10.71	34.74	41.07	8.16	0.65	1.08	0.90	0.19	1.11
LD02-4	6.98	32.39	15.59	14.67	5.21	4.22	2.54	18.39	4.20	2.36	0.17	1.07
LD03-1	0.03	0.86	1.35	0.43	16.86	55.56	24.27	0.65	0.45	0.64	0.04	0.99
LD03-2	2.47	4.62	33.89	55.62	1.14	0.00	0.00	2.26	2.93	0.85	0.36	2.59
LD03-3	1.91	6.91	14.63	23.86	27.58	20.40	1.53	3.18	2.04	1.54	0.26	1.27
LD03-4	7.26	19.24	17.90	23.73	15.20	8.16	0.59	7.92	3.42	2.19	0.34	1.16

Note: clay,  $<5\ \mu\text{m}$ ; silt,  $5\text{--}63\ \mu\text{m}$ ; VFS, very fine sand,  $63\text{--}125\ \mu\text{m}$ ; FS, fine sand,  $125\text{--}250\ \mu\text{m}$ ; MS, medium sand,  $250\text{--}500\ \mu\text{m}$ ; CS, coarse sand,  $500\text{--}1000\ \mu\text{m}$ ; VCS, very coarse sand,  $1000\text{--}2000\ \mu\text{m}$ .  $M_z$ , mean grain-size;  $\sigma_1$ , sorting;  $SK_1$ , skewness;  $K_g$ , kurtosis. BD, barchan dunes; LD, linear dunes.

##### 3.1.2 Frequency curve

Figure 4 shows the frequency curves for the samples. Two barchan dunes (BD01 and BD02) developed in the alluvial fans of the Lvliang Mountains, showed a unimodal distribution, with the main peak between 200 and 300  $\mu\text{m}$ . Their cumulative frequency curves exhibited a single segment that represents the saltation load (i.e., all particles between 100 and 500  $\mu\text{m}$ ). In contrast, frequency curve for the third barchan dune (BD03), which developed in the dry salt flats in the Sebei area (Fig. 2), displayed a bimodal distribution, with the main peak between 300 and 500  $\mu\text{m}$  and a secondary peak between 40 and 60  $\mu\text{m}$ , which formed a fine tail. Cumulative frequency curve for this dune showed two segments, which represented the modified saltation load (i.e.,

particles between 63 and 100  $\mu\text{m}$ ) and the saltation load, respectively, and the boundary between these two loads occurred near 120  $\mu\text{m}$  (Fig. 4).

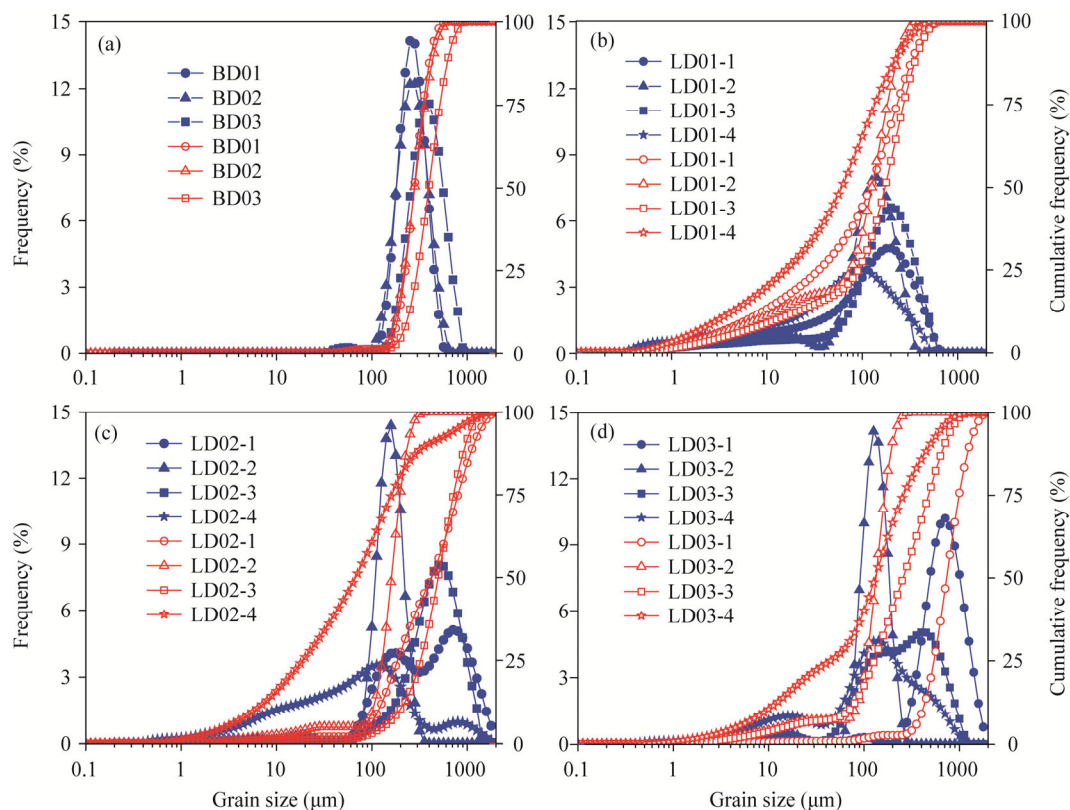


**Fig. 4** Grain-size frequency (blue line) and cumulative frequency (red line) curves for dune surface sediments

Grain-size distribution curves for different positions on and near linear dunes (LD01–LD03) differed greatly. Frequency curves for crest sediments showed an obvious bimodal distribution with the main peak between 100 and 200  $\mu\text{m}$  and a secondary peak between 10 and 20  $\mu\text{m}$ , which represent the saltation load and suspension load, respectively. Suspension load formed a fine tail similar to that of barchan dune in the dry salt flats. Their cumulative frequency curves also included two segments, with the suspension load showing a gentle slope and the saltation load showing a steep slope. Frequency curves for sediments at the toe of dune slopes also exhibited a bimodal distribution, but with their main peak between 200 and 500  $\mu\text{m}$  and the secondary peak between 20 and 100  $\mu\text{m}$ , which represent the saltation load and suspension/modified saltation load. Their cumulative frequency curves also consisted of two segments. The obvious difference from dune crest distribution is that the suspension and modified saltation loads were mixed for sediments at slope toes. Grain-size distribution curves for inter-dune sediments were more complex. Their frequency curves were wider and flatter, and showed an obvious bimodal distribution. Most of cumulative frequency curves included two segments, but the points that marked the boundaries among suspension, modified saltation and saltation loads were ambiguous, which indicated that sorting of inter-dune sediments was poor (Fig. 4).

### 3.1.3 Grain-size parameter

Figure 5 shows the relationships between  $M_z$  and other grain-size parameters for the dunes that are summarized in Table 1. In summary, these relationships differed among dune types and sample positions. With the coarsening of  $M_z$  for dune surface sediments, their  $\sigma_1$  gradually increased and  $SK_1$  changed from strongly positively skewed to a nearly symmetrical distribution, whereas  $K_g$  showed no obvious trend as a function of grain-size. The  $\sigma_1$  was the strongest for

barchan dunes that developed in the alluvial fans, followed by barchan dunes in the dry salt flats, whereas linear dunes had the poorest sorting. Grain-size frequency curves for barchan dunes and SSW slope sample of linear dune LD03 showed nearly symmetrical distributions. However, grain-size frequency curves of other sediments showed a positively skewed distribution with a fine tail, especially for LD01, and these patterns may have been influenced by underlying terrain.

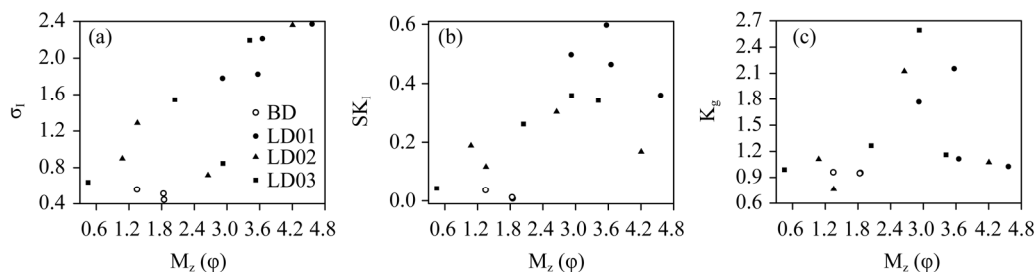


**Fig. 5** Grain-size parameters ( $\sigma_i$ , sorting (a);  $SK_i$ , skewness (b);  $K_g$ , kurtosis (c)) for dune surface sediments as a function of mean particle size ( $M_z$ )

### 3.2 Soluble salt content

Table 1 shows an obvious contrast in soluble salt contents for dunes on two types of underlying terrain. Soluble salt contents of barchan dunes in the alluvial fans of the Lvliang Mountains ranged between 0.03% and 0.13%. And soluble salt content of barchan dune in the dry salt flats near Sebei area reached 0.90%. In contrast, soluble salt contents of linear dunes were much higher. At sampling position LD01, soluble salt contents ranged between 5.09% and 10.83%, versus between 0.65% and 18.39% at LD02 and between 0.65% and 7.92% at LD03. Salt contents also differed among positions, with values ranging between 0.65% and 9.14% at toe, between 1.42% and 5.09% at dune crest, and between 7.92% and 18.39% in inter-dune areas. These results showed that soluble salt contents were the highest in inter-dune areas, followed by dune crest, with slope toes having the lowest values. This result can be attributed to the higher contents of coarser grains at the toe of linear dune slope (Table 1), which have a lower surface area and therefore hold a smaller amount of soluble salts.

Soluble salts can bind silt and clay particles together, thereby increasing the cohesion of dune sediments. Therefore, soluble salt contents in underlying terrain can potentially control dune development through their effect on cohesion. Figure 6 shows the relationship between total content of silt, clay particles and soluble salts for dune surface sediments. Total contents of silt, clay particles and soluble salts for barchan dunes range between 0.03% and 1.81%, with a mean value of 0.65%. In contrast, soluble salt contents for different positions on and around the linear dunes ranged widely, between 1.53% and 39.70%, and averaged 13.85%. Total contents of silt, clay particles and soluble salts were the highest for inter-dune sediments, with a mean value of 49.48% and a range between 34.42% and 57.77%. There was a strong and statistically significant negative relationship between total content of silt, clay particles and soluble salts.

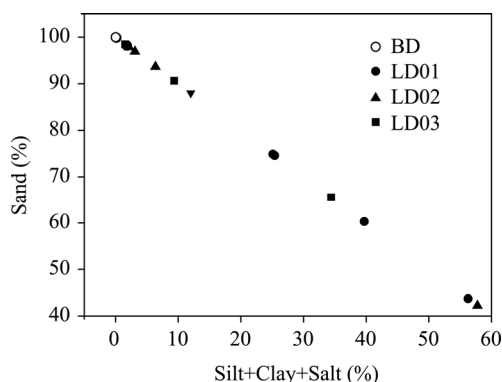


**Fig. 6** Relationship between sand content and total content of silt, clay and salt

### 3.3 Micro-textures of quartz sand grains

#### 3.3.1 Roundness

Roundness of quartz sand grains provides abundant information on the exogenic agents that shaped their evolution and transport distance. Based on their appearance, we divide roundness of quartz sand grains into rounded, sub-rounded, sub-angular and angular. Generally speaking, rounded and sub-rounded quartz sand grains have been transported a long distance or by strong hydrodynamic forces, since repeated impacts with other particles tends to remove angular parts of the surface, and the amount of rounding increases with transport distance or flow strength. Sub-angular and angular quartz sand grains, which have retained at least some of their angular features, have typically been transported a relatively short distance or by weak hydrodynamic forces, or may have been shaped by glaciation. Quartz sand grains that developed in an aeolian environment are usually well rounded, whereas those that developed in an aqueous environment usually have medium to slight roundness. Roundness of quartz sand grains formed in a glacial environment is the poorest.

Roundness of quartz sand grains was poor, as they were dominated by sub-angular and angular grains, and contents of sub-rounded and rounded grains were relatively low (Table 2). Dune sands at the crest of barchans were mainly composed of sub-angular grains, with an average of 41.27%. Sub-rounded grains were the second-most abundant, with an average of 38.37%, followed by 10.32% and 10.05% for angular and rounded grains, respectively. Linear dunes were also mainly composed of sub-angular grains, with an average of 42.23%. This was followed by the contents of angular and sub-rounded grains, with the values of 28.45% and 24.88%, respectively, and the content of rounded grains was only 4.45%. Roundness was the poorest for inter-dune sediments, with total content of angular and sub-angular grains reaching 80.75% and contents of sub-rounded and rounded grains totaling only 19.25%.

**Table 2** Frequency of roundness features of quartz sand grains for dune surface sediments

Sample	Rounded (%)	Sub-rounded (%)	Sub-angular (%)	Angular (%)
BD01 ( $n=28$ )	21.43	32.14	32.14	14.29
BD02 ( $n=22$ )	4.55	45.45	50.00	0.00
BD03 ( $n=24$ )	4.17	37.50	41.67	16.67
LD01-1 ( $n=48$ )	0.00	29.17	41.67	29.17
LD01-2 ( $n=32$ )	3.13	37.50	40.63	18.75
LD01-3 ( $n=33$ )	12.12	42.42	18.18	27.27
LD01-4 ( $n=50$ )	0.00	26.00	48.00	26.00
LD02-1 ( $n=35$ )	5.71	11.43	48.57	34.29
LD02-2 ( $n=44$ )	0.00	6.82	38.64	54.55
LD02-3 ( $n=21$ )	19.05	14.29	38.10	28.57
LD02-4 ( $n=38$ )	0.00	18.42	55.26	26.32
LD03-1 ( $n=10$ )	0.00	50.00	40.00	10.00
LD03-2 ( $n=38$ )	0.00	10.53	44.74	44.74
LD03-3 ( $n=23$ )	0.00	21.74	69.57	8.70
LD03-4 ( $n=30$ )	3.33	10.00	30.00	56.67

Note: BD, barchans; LD, linear dunes.

#### 3.3.2 Surface micro-textures

Surface micro-textures on quartz sand grains provide insights into the sedimentary history of clastic sediments and their transport agents. Crescent- and dish-shaped depressions, pockmarked pits and upturned cleavage plates are common for quartz sand grains that developed in an aeolian



environment. Conchoidal fractures are well developed for quartz sands that developed in a glacial environment, and cleavage planes, striation and impact pits are also common. In contrast, quartz sand grains that developed in a subaqueous environment usually develop a polished surface, with V-shaped depressions and straight or bent impact grooves. Quartz sand grains that developed in a chemical environment (i.e., an environment with strong chemical reactions) usually form corresponding solution and precipitation structures. For example, grains that developed in an environment where  $\text{SiO}_2$  solution is strong usually develop pits, grooves and scaly exfoliation. In contrast, the precipitation of  $\text{SiO}_2$  usually forms siliceous spheres, scales, films or botryoidal precipitate micro-structures (Table 3; Fig. 7).

By thoroughly analyzing the scanning electron micrographs, we found all of the micro-textures produced by mechanical transport by glacial, fluvial and aeolian forces, as well as the results of  $\text{SiO}_2$  solution and precipitation on the surface of quartz sand grains (Fig. 7). However, the combination and occurrence frequency of specific micro-textures differed greatly among the dune sands from different environments and dune types (Fig. 8). Barchan dunes (BD01 and BD02) that developed in the alluvial fans of the Lvliang Mountains were dominated by micro-textures produced by aeolian transport. Occurrence frequency of crescent- and dish-shaped depressions was much higher. Micro-textures produced by glacial and fluvial forces were the second most frequent, and micro-textures that developed in a chemical environment were much less frequent. These micro-textures indicate that alluvial sediments in the piedmont of the Lvliang Mountains were transported by glacial and fluvial forces, and then deposited at the foot of mountain slopes. Sand-sized particles then transformed into barchan dunes under the influence of wind (i.e., aeolian transport). V-shaped depressions and subaqueous polished surfaces caused by fluvial transport were the most common in the Sebei area. Typical micro-textures caused by aeolian transport, such as dish- and crescent-shaped depressions, also occurred at a high frequency, which indicates a strong aeolian environment. In addition, micro-textures of quartz sand grains in chemical environment were well developed compared with barchans in the alluvial fans, which suggests that those quartz sand grains developed in a much warmer paleoclimate. Hence, dune sands of barchan in the Sebei area probably first experienced short-distance glacial transport, followed by long-distance transport of strong hydrodynamic forces. Besides, these dune sands also evolved under strong aeolian transport combined with chemical etching and precipitation, because the climate of the Sebei area is characterized by strong winds and their underlying terrain is characterized by a high content of soluble salts.

Although linear dunes contained particles with all the surface micro-textures caused by glacial, fluvial, aeolian and chemical forces, the occurrence frequency of micro-textures caused by chemical forces was much higher than that of barchan dunes (Fig. 8). This result can be attributed to the short distance of linear dunes to the Qarhan Salt Lake. At sample location LD01,

**Table 3** Relationship between surface micro-textures of quartz sand grains and exogenic agents responsible for these features

Sedimentary environment		Micro-texture and corresponding code
Mechanical erosion	Glacial environment	Conchoidal fracture-1, cleavage plane-2, striation-3, impact pits-4
	Subaqueous environment	Subaqueous polished surface-5, V-shaped depression-6, straight impact groove-7, bent impact groove-8
	Aeolian environment	Crescent-shaped depression-9, dish-shaped depression-10, pockmarked pit-11, upturned cleavage plate-12
Chemical environment	$\text{SiO}_2$ solution	Solution pits-13, solution grooves-14, scaly exfoliation-15
	$\text{SiO}_2$ precipitation	Siliceous sphere-16, siliceous scale-17, siliceous film-18, botryoidal precipitate of $\text{SiO}_2$ -19

Note: Numbers refer to the microphotographs in Figure 7 that shows these features.

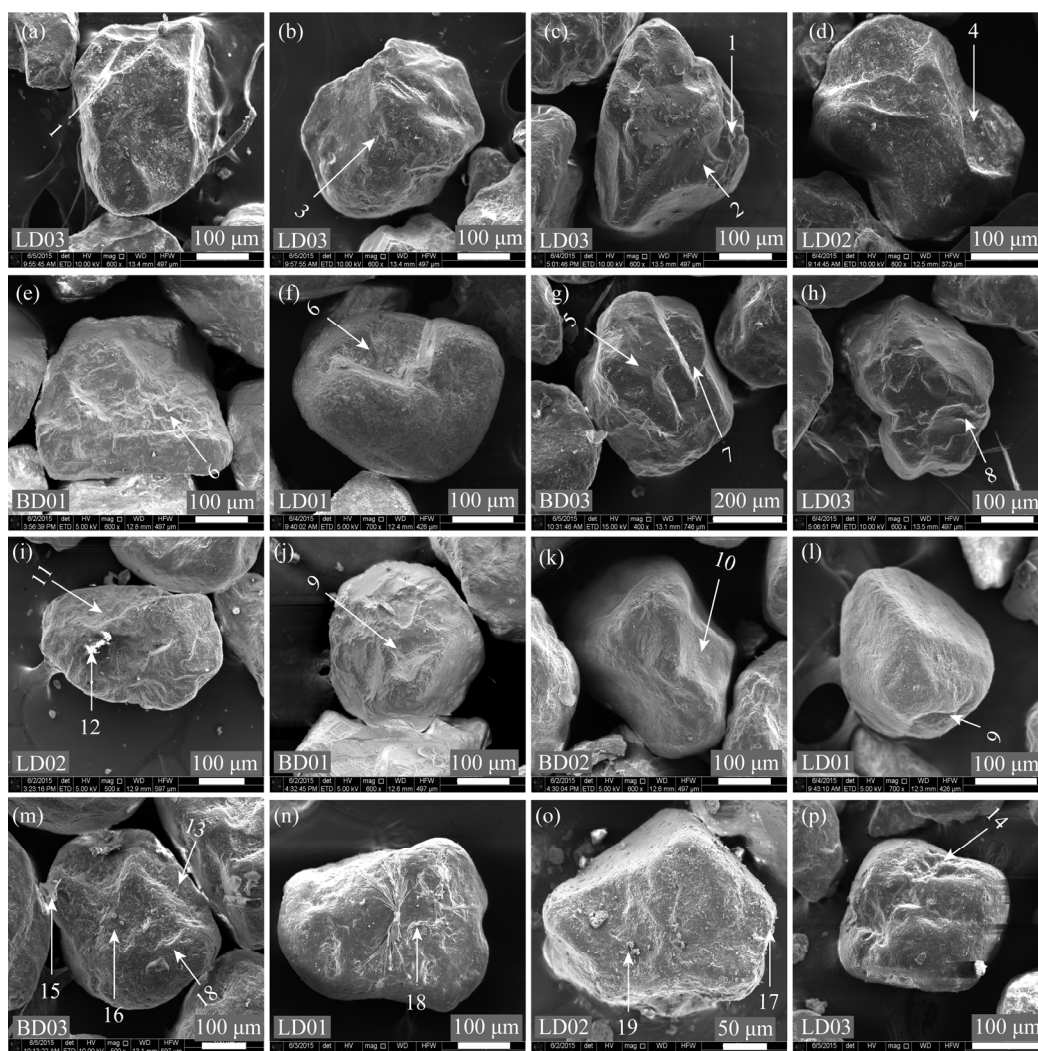


**Fig. 7** Surface micro-textures of quartz sand grains for sand dune sediments. The connotations of the numbers are explained in Table 3.

the frequency of surface micro-textures caused by aeolian transport, such as crescent- and dish-shaped depressions, accounted for 40.97% of the total, followed by V-shaped depressions and straight impact grooves (29.60%), which were produced by fluvial forces. Occurrence frequencies of micro-textures caused by chemical and glacial forces totaled 15.87% and 13.56%, respectively. Patterns and frequencies for quartz sand grains sampled at locations LD02 and LD03 were similar to those at location LD01. At sample location LD02, the frequency of micro-textures caused by aeolian transport was obviously higher than those at the other sites, which can be attributed to a longer distance of transport by wind. At sample location LD03, occurrence frequency of micro-textures caused by chemical processes was higher than those of the other sediments, which can be ascribed to the location of these dune sands on the northern margin of the Qarhan Salt Lake (Fig. 2). Meltwater from ice and snow can expand the lake's area in the spring, and the water can even enter into inter-dune areas (Fig. 9). Thus, soluble salts can concentrate at the surface of formerly dry salt flats under capillary action, leading to strong chemical etching and precipitation in dune sands near the salt lake. In addition, the occurrence frequency of micro-textures caused by fluvial forces was slightly higher than those of the other sites. This suggests that sands of linear dunes were first transported into the basin by glacial and fluvial processes, and then wind transported these sands to their current locations in the salt flats, where chemical etching and precipitation occurred.

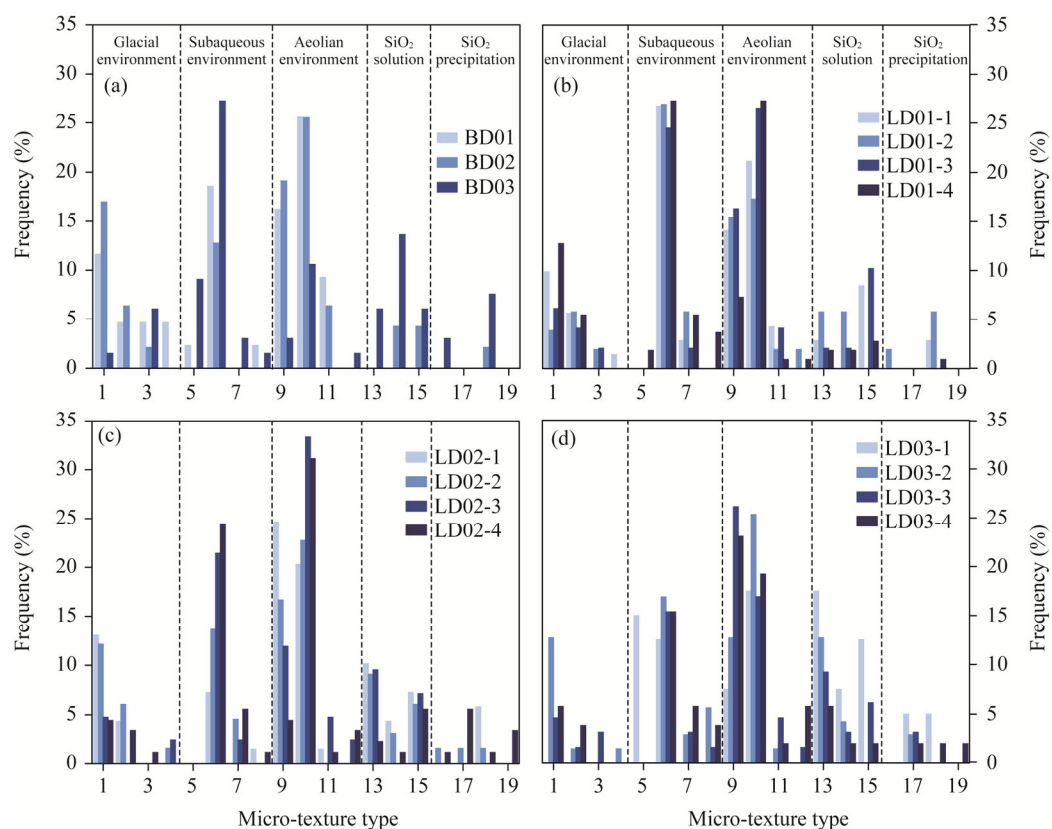


**Fig. 8** Frequency of surface micro-textures on quartz sand grains. Table 3 defines the meaning of the numbers for micro-texture type and Figure 7 illustrates these features.



**Fig. 9** Lake water that has entered inter-dune area in the field of linear dunes during spring melting of snow and ice

## 4 Discussion

### 4.1 Influence of underlying terrain on dune development

Formation and development of aeolian dunes are influenced by local wind regime, sand supply and underlying terrain (Pye and Tsoar, 2009). The Qaidam Basin is a closed inland fault basin, and northerly and northwesterly winds are the dominant aeolian forces in the basin. Linear and barchan dunes in the Sebei area developed under a broad unimodal wind regime (Li et al., 2020), whereas barchan dunes in the piedmont of the Lvliang Mountains were mainly influenced by northwesterly winds (Fig. 3a). These two dune types coexist in the western part of the Qarhan Salt

Lake (Lü et al., 2018). Therefore, wind regime cannot by itself explain the formation of the barchan and linear dunes. Aeolian sands in the Qaidam Basin mainly originated from fluvial and lacustrine sediments (Bao and Dong, 2015; Du et al., 2018), so barchan and linear dunes are of similar provenance. However, the underlying terrain for both dune types was quite distinct. Barchan dunes are mainly distributed in the alluvial fans of the surrounding mountains, whereas linear dunes are mainly distributed in the dry salt flats of modern salt lakes. Although barchan dunes in the Sebei area developed in the dry salt flats of ancient lakes, soluble salt content in their crests was similar to that in barchan dunes that developed in the alluvial fans. However, the soluble salt content of linear dunes was much higher than that of barchan dunes, especially in the inter-dune area, where the values can be hundreds of times that for barchans (Table 1).

Soluble salt contents in the surfaces of alluvial fans and dry salt flats of ancient lakes were much lower than those in the other locations. The underlying terrain of both types are flat with a limited supply of loose sand. Therefore, barchan dunes developed under the influence of a unimodal wind regime (Wasson and Hyde, 1983). In contrast, dry salt flats around modern salt lakes allow soluble salts to become concentrated at the surface under the influence of running water and evaporation. Silt and clay contents were also much higher in the surface sediments of salt flats (Table 1). Both factors make these sediments more cohesive. When the wind carries loose sand and salt particles to the modern dry salt flats, these particles are captured by the underlying cohesive finer particles, leading to the formation of initial topographic obstacles around which the dunes formed. With a continuous supply of loose sediments and unimodal wind regime, these obstacles gradually grew in length and height, and eventually developed into linear dunes (Rubin and Hesp, 2009). Hence, our results suggest that different environmental settings especially differences in soluble salts contents in underlying terrain were important factors that determined the types of dunes that developed.

#### 4.2 Transport pathways and sedimentary environments for dune sands

Denudation clastic sediments from surrounding mountains that produced by weathering are the ultimate provenance of various aeolian depositional landforms in the Qaidam Basin. However, exogenic agents transported these sediments cannot be confirmed until the quartz sand grains eventually accumulated into dunes. Because of widespread distribution of quartz sand grains and their physical and chemical stability, their surface micro-textures, which are produced by mechanical erosion caused by exogenic agents as well as by chemical etching and precipitation, can remain visible for a long time on the surface of quartz sand grains (Vos et al., 2014). Thus, these particles bear abundant information on their transport agents and sedimentary environments. Micro-textures caused by glacial forces, such as conchoidal fractures and cleavage planes, can be found on the quartz sand grains in all of the sediment samples. However, these samples were weakened in some samples, which indicated that the dune sands underwent glacial transport before they entered into the basin (Gao et al., 1995). Glacial tills became concentrated in erosion channels in the mountainous areas under the action of gravity and slope runoff. They were then transported by running water and deposited in the piedmont of mountains to form alluvial fans, during which time micro-textures caused by fluvial forces, such as V-shaped depressions and straight and bent impact grooves, became well developed. With the continuous uplift of surrounding mountains since the late Pleistocene, the lakes in the basin gradually dried up and the climate became arid and windy. Sand-sized particles preserved near the dried lakes, ancient channels and alluvial fans were then transported by northerly and northwesterly winds and eventually developed into various dune types. During this transport, the typical aeolian surface micro-textures of crescent- and dish-shaped depressions as well as pockmarked pits produced by aeolian transport became well developed.

Dune sands in the Qaidam Basin have been transported by glacial, fluvial and aeolian processes in sequence. However, their overall roundness was poor (Table 2). On the one hand, this can be attributed to the shorter flow paths for the inland rivers in the basin (Zhang and Liu, 1985); on the other hand, the dunes are close to their source regions. Despite these similarities, the chemical



processes that acted on the quartz sand grains showed distinct differences between underlying terrain types. The overall surface of quartz sand grains distributed in the alluvial fans showed fewer signs of long-term modification, which suggests that the particles were recently deposited. The surface micro-textures, such as solution grooves, scaly exfoliation and siliceous films that indicated a low-energy chemical environment were only found on the surface of some quartz sand grains. However, the micro-textures of pits, grooves and scaly exfoliation caused by  $\text{SiO}_2$  solution, and the siliceous scales and siliceous films caused by  $\text{SiO}_2$  precipitation were well developed for quartz sand grains in the dry salt flats, which represented a high-energy chemical environment.

## 5 Conclusions

Based on the grain-size data, soluble salt contents and surface micro-textures of quartz sand grains in the Qaidam Basin, we explored the influence of underlying terrain on dune sands. Barchan dunes were dominated by medium sands, and their frequency curves for barchan dunes showed a unimodal distribution pattern, dominated by saltation load. In contrast, linear dunes were mainly composed of fine sands, and their frequency curves showed a bimodal distribution, with the main peak represented saltation load and the secondary peak represented modified saltation load or suspension load. Soluble salt contents of linear dunes that developed in the salt flats were much higher than those of barchan dunes that developed in the alluvial fans. The overall roundness of dune sands in the Qaidam Basin was poor, with the sands dominated by sub-angular and angular particles. This suggested that dune sands were transported over a relatively short distance by exogenic agents. Surface micro-textures of quartz sand grains indicated that they were transported by glacial, fluvial and aeolian processes successively, and eventually deposited at their current location, where they evolved into dunes. Alluvial fans below mountains represented a low-energy chemical environment, so the micro-textures caused by chemical etching and precipitation were not well developed for quartz sand grains in these barchan dunes. In contrast, salt flats had a high-energy chemical environment, and the micro-textures introduced by chemical etching and precipitation were well developed for quartz sand grains in linear dunes.

## Acknowledgements

The study was funded by the National Natural Science Foundation of China (41601005, 41930641) and the Scientific and Technological Innovation Programs of Higher Education Institutions in Shanxi Province (2019L0797). We appreciate the constructive and insightful comments from two anonymous reviewers who greatly improved the manuscript.

## References

- Bao F, Dong Z B. 2015. Mineral composition and origin of surface sediment in the desert of the Qaidam Basin. *Journal of Northwest University*, 45(1): 90–96. (in Chinese)
- Bristow C, Livingstone I. 2019. Dune sediments. In: Livingstone I, Warren A. *Aeolian Geomorphology*. Chichester: John Wiley & Sons, 209–236.
- Chen B X, Lü M Q. 1959. Aeolian landforms in the Qaidam Basin. *Journal of Nanjing University*, (6): 35–42. (in Chinese)
- Dong Z B, Wang T, Wang X M. 2004. Geomorphology of the megadunes in the Badain Jaran Desert. *Geomorphology*, 60(1–2): 191–203.
- Dong Z B, Wei Z H, Qian G Q, et al. 2010. "Raked" linear dunes in the Kumtagh Desert, China. *Geomorphology*, 123(1–2): 122–128.
- Dong Z B, Hu G Y, Qian G Q, et al. 2017a. High-altitude aeolian research on the Tibetan Plateau. *Reviews of Geophysics*, 55(4): 864–901.
- Dong Z B, Lu J H, Qian G Q, et al. 2017b. *Tibetan Plateau Atlas of Aeolian Geomorphology*. Xi'an: Xi'an Map Press, 14–37. (in Chinese)
- Du S S, Wu Y Q, Tan L H. 2018. Geochemical evidence for the provenance of aeolian deposits in the Qaidam Basin, Tibetan



- Plateau. *Aeolian Research*, 32: 60–70.
- Folk R L, Ward W C. 1957. Brazos River bar: a study in the significance of grain size parameters. *Journal of Sedimentary Research*, 27(1): 3–26.
- Gao C H, Mu G J, Yan S, et al. 1995. Features of surface microtextures of quartz sand grains in the hinterland of the Taklimakan Desert and their environmental significance. *Geological Review*, 41(2): 152–158. (in Chinese)
- Garzanti E, Vermeesch P, Andò S, et al. 2013. Provenance and recycling of Arabian desert sand. *Earth-Science Reviews*, 120: 1–19.
- Han W X, Ma Z B, Lai Z P, et al. 2014. Wind erosion on the north-eastern Tibetan Plateau: constraints from OSL and U-Th dating of playa salt crust in the Qaidam Basin. *Earth Surface Processes and Landforms*, 39(6): 779–789.
- Hu F G, Yang X P. 2016. Geochemical and geomorphological evidence for the provenance of aeolian deposit in the Badain Jaran Desert, northwestern China. *Quaternary Science Reviews*, 131: 179–192.
- Kocurek G, Lancaster N. 1999. Aeolian system sediment state: theory and Mojave Desert Kelso dune field example. *Sedimentology*, 46(3): 505–515.
- Krinsley D H, Doornkamp J C. 1973. *Atlas of Quartz Sand Surface Textures*. Cambridge: Cambridge University Press, 1–91.
- Lancaster N. 2013. Sand seas and dune fields. In: Shroder J, Lancaster N, Sherman D J, et al. *Treatise on Geomorphology*. San Diego: Academic Press, 219–245.
- Lancaster N, Baker S, Bacon S, et al. 2015. Owens Lake dune fields: composition, sources of sand, and transport pathways. *CATENA*, 134: 41–49.
- Li J Y, Dong Z B, Zhang Z C, et al. 2015. Grain-size characteristics of linear dunes on the northern margin of Qarhan Salt Lake, northwestern China. *Journal of Arid Land*, 7(4): 438–449.
- Li J Y, Dong Z B, Qian G Q, et al. 2016. Yardangs in the Qaidam Basin, northwestern China: distribution and morphology. *Aeolian Research*, 20: 89–99.
- Li J Y, Zhao E D, Liu W L. 2018. Provenance and transport pathways of linear dunes in the northern margin of Qarhan Salt Lake of China. *Journal of Desert Research*, 38(5): 909–918. (in Chinese)
- Li J Y, Zhou L, Yan J L, et al. 2020. Source of aeolian dune sands on the northern margin of Qarhan Salt Lake, Qaidam Basin, NW China. *Geological Journal*, 55(5): 3643–3653.
- Lü P, Dong Z B, Rozier O. 2018 The combined effect of sediment availability and wind regime on the morphology of aeolian sand dunes. *Journal of Geophysical Research: Earth Surface*, 123(11): 2878–2886.
- Muhs D R, Reynolds R L, Been J. 2003. Aeolian sand transport pathways in the southwestern United States: importance of the Colorado River and local sources. *Quaternary International*, 104(1): 3–18.
- Powers M C. 1953. A new roundness scale for sedimentary particles. *Journal of Sedimentary Petrology*, 23(2): 117–119.
- Pye K, Tsoar H. 2009. *Aeolian Sand and Sand Dunes*. Berlin: Springer, 141–173.
- Qian G Q, Yang Z L, Luo W Y, et al. 2020. Morphological and sedimentary characteristics of dome dunes in the northeastern Qaidam Basin, China. *Geomorphology*, 350: 106923, doi: 10.1016/j.geomorph.2019.106923.
- Qian Z Y. 1986. Investigations on the sand harm to Qinghai-Xizang railway in Yanqiao area and sand control plan. *Journal of Desert Research*, 6(2): 27–30.
- Rubin D M, Hesp P A. 2009. Multiple origins of linear dunes on Earth and Titan. *Nature Geoscience*, 2: 653–658.
- Scheidt S, Lancaster N, Ramsey M. 2011. Eolian dynamics and sediment mixing in the Gran Desierto, Mexico, determined from thermal infrared spectroscopy and remote-sensing data. *Geological Society of America Bulletin*, 123(7–8): 1628–1644.
- Vos K, Vandenbergh N, Elsen J. 2014. Surface textural analysis of quartz grains by scanning electron microscopy (SEM): From sample preparation to environmental interpretation. *Earth-Science Reviews*, 128: 93–104.
- Wasson R J, Hyde R. 1983. Factors determining desert dune type. *Nature*, 304: 337–339.
- Wu Z. 2010. *Geomorphology of Wind-drift Sands and Their Controlled Engineering*. Beijing: Science Press, 236–286. (in Chinese)
- Xie Y Y. 1984. *Atlas of Quartz Sand Surface Textural Features of China Micrographs*. Beijing: China Ocean Press, 1–148. (in Chinese)
- Xu Z W, Lu H Y, Zhao C F, et al. 2010. Composition, origin and weathering process of surface sediment in Kumtagh Desert, northwest China. *Acta Geographica Sinica*, 65(1): 53–64. (in Chinese)
- Yu L P, Lai Z P. 2012. OSL chronology and palaeoclimatic implications of aeolian sediments in the eastern Qaidam Basin of the northeastern Qinghai-Tibetan Plateau. *Palaeogeography, Palaeoclimatology, Palaeoecology*, 337–338: 120–129.
- Yu L P, Lai Z P. 2014. Holocene climate change inferred from stratigraphy and OSL chronology of aeolian sediments in the Qaidam Basin, northeastern Qinghai-Tibetan Plateau. *Quaternary Research*, 81(3): 488–499.
- Yu L P, Lai Z P, An P, et al. 2015. Aeolian sediments evolution controlled by fluvial processes, climate change and human activities since LGM in the Qaidam Basin, Qinghai-Tibetan Plateau. *Quaternary International*, 372: 23–32.

- Zeng Y N, Feng Z D, Cao G C. 2003. Desert formation and evolution in Qaidam Basin since the last glacial epoch. *Acta Geographica Sinica*, 58(3): 452–457. (in Chinese)
- Zhang C, Li Z L, Chen Q J, et al. 2020. Provenance of aeolian sands in the Ulan Buh Desert, northwestern China, revealed by heavy mineral assemblages. *CATENA*, 193: 104624, doi: 10.1016/j.catena.2020.104624.
- Zhang J Z, Liu E B. 1985. Hydrological characteristics of streams in Qaidam Basin. *Acta Geographica Sinica*, 52(3): 242–255. (in Chinese)
- Zhang Z C, Dong Z B, Qian G Q, et al. 2018. Formation and development of dunes in the northern Qarhan Desert, central Qaidam Basin, China. *Geological Journal*, 53(3): 1123–1134.
- Zhou J X, Zhu Y, Yuan C Q. 2012. Origin and lateral migration of linear dunes in the Qaidam Basin of NW China revealed by dune sediments, internal structures, and optically stimulated luminescence ages, with implications for linear dunes on Titan. *GSA Bulletin*, 124(7–8): 1147–1154.
- Zhu Z D, Wu Z, Liu S, et al. 1980. *An Outline of Chinese Desert*. Beijing: Science Press, 77–78. (in Chinese)